Vacuum sublimed α,ω-dihexylsexithiophene thin films: Correlating electronic structure and molecular orientation

S. Duhm,[1] I. Salzmann,[1] N. Koch,[1,a)] H. Fukagawa,[2] T. Kataoka,[2] S. Hosoumi,[2] K. Nebashi,[2] S. Kera,[2] and N. Ueno[2]
[1]*Institut für Physik, Humboldt-Universität zu Berlin, Newtonstr. 15, D-12489 Berlin, Germany*
[2]*Graduate School of Advanced Integration Science, Chiba University, 1-33 Yayoi-cho, Inage-ku, Chiba 263-8522, Japan*

(Received 23 April 2008; accepted 12 June 2008; published online 15 August 2008)

In order to correlate the molecular orientation of organic thin films with charge injection barriers at organic/metal interfaces, the electronic structure and molecular orientation of vacuum sublimed thin films of α,ω-dihexylsexithiophene (DH6T) on the substrates Ag(111), highly oriented pyrolytic graphite (HOPG), and tetratetracontane (TTC) precovered Ag(111) were investigated. Results from metastable atom electron spectroscopy, ultraviolet photoelectron spectroscopy, and x-ray diffraction were used to derive growth models (including molecular orientation and conformation) of DH6T on the different substrates. On Ag(111), DH6T exhibits a transition from lying molecules in the monolayer/bilayer range to almost standing upright molecules in multilayers. This is accompanied by a shift of the molecular energy levels to a lower binding energy by 0.65 eV with respect to the vacuum level. The unit cell of standing DH6T on lying DH6T on Ag(111) is estimated to be similar to the DH6T bulk phase. On HOPG, DH6T grows in the bulk phase with lying orientation, starting already from the monolayer coverage. DH6T on TTC precovered Ag(111) grows in an almost lying orientation and a conformation that allows a strong overlap of the hexyl chains of DH6T with the alkyl chains of TTC. In all cases, the electronic structure and, particulary, the ionization energy of DH6T is dependent on the orientation of DH6T, i.e., lying DH6T has higher ionization energy than standing DH6T. © *2008 American Institute of Physics*. [DOI: 10.1063/1.2968254]

I. INTRODUCTION

The molecular orientation of organic thin films impacts numerous physical properties, such as charge injection, photoluminescence, and the transport properties of these thin films.[1–4] Therefore, the molecular orientation, which itself is strongly dependent on the substrate-adsorbate interaction,[5,6] directly impacts the performance of devices composed of thin organic films in the field of *organic electronics*.[7–9] In such organic thin films, usually standing rigid rodlike conjugated organic molecules (COMs) exhibit a lower ionization energy (IE) than lying molecules.[10–13] As recently shown, this orientation dependent IE in molecular assemblies can be explained by a macroscopic impact of intramolecular surface dipoles on the potential around the molecular assembly,[14] a concept similar to the orientation dependent work function of metal single crystals. In COMs, the π-electron system of the conjugated backbone above and below the molecular midplane is clearly negatively charged, compensated by a positively charged midplane of the molecule, leading to an intramolecular dipole moment perpendicular to the π-system plane. For flat lying rigid rodlike COMs on a substrate, this dipole moment is parallel to the film surface normal. Whereas for standing COMs, the mostly (depending on the endgroup termination) nonpolar long axis endgroups compose the surface, which leads to the observed phenomenon of lower IE in standing molecules compared to lying molecules. IE is correlated with the charge injection barriers at the organic/metal interface. In the case of vacuum level alignment, this correlation is even linear.[15,16] Therefore, achieving control over the molecular orientation allows the lowering of the hole injection barrier (HIB), which is a crucial parameter for device performance,[7–9] e.g., by a transition from flat lying COMs to standing COMs. Thin films of the hexyl chain substituted sexithiophene (6T) derivate α,ω-dihexylsexithiophene (DH6T) (Refs. 17–19) exhibit interesting properties. DH6T on Ag(111) undergoes an orientational transition from flat lying molecules [lying layer (LL)] in the monolayer regime to almost standing molecules [standing layer (SL)] in the multilayer.[13] This transition is accompanied by a shift in the molecular levels toward lower binding energies (BEs) and by a lowering in the HIB of 0.60 eV at the monolayer/multilayer homointerface.[14] Moreover, thin layers of DH6T on metal substrates have the capability to influence the growth mode of 6T that is deposited on top. On metal substrates, 6T grows with its long molecular axis parallel to the substrate surface up to a film thickness of several hundred layers,[20,21] which can be deliberately changed to a standing growth mode for the first layer by prepatterning the metal with a layer of standing DH6T.[14] This offers the possibility to lower the 6T HIB through control of the molecular orientation.

However, the driving force for the change in molecular orientation of DH6T is not yet well understood. Therefore, it is of interest from a fundamental point of view to study the morphology and the electronic structure of DH6T on different substrates selected according to distinct physical properties. In this work, we used ultraviolet photoelectron spectros-

a)Electronic mail: norbert.koch@physik.hu-berlin.de.

copy (UPS) *in situ* combined with metastable atom electron spectroscopy (MAES) as a main experimental tool. In MAES, the sample is excited with metastable He^* atoms that do not penetrate the sample surface and, hence, just probe the outermost occupied molecular orbitals of an organic thin film. In combination with quantum-chemical calculations of the molecular orbitals, the molecular orientation can be determined from the MAES measurements.[22,23] We performed the experiments on substrates with different physical properties, with Ag(111) as metallic reference substrate, highly oriented pyrolytic graphite (HOPG) as weakly interacting but metalliclike substrate, and Ag(111) precovered with tetratetracontane (TTC), which is a long alkyl chain and forms highly ordered monolayers on Ag(111).[24,25] The latter substrate was chosen to investigate the role of the alkyl chains on the process of orientational transition of DH6T on Ag(111). In addition to the spectroscopic methods, x-ray reflectivity (XRR) and grazing incidence x-ray diffraction (GID) measurements were performed on the thin DH6T films on Ag(111) in order to support the structural information deduced from electron spectroscopy.

II. EXPERIMENTAL

UPS and MAES experiments were performed using an apparatus described in detail elsewhere.[26] The interconnected sample preparation (base pressure of 3×10^{-10} mbar) and analysis chambers (base pressure of 2×10^{-10} mbar) allowed sample transfer without breaking the ultrahigh vacuum conditions. The Ag(111) single crystal was cleaned by repeated Ar-ion sputtering and annealing cycles (up to 550 °C). The crystal quality was checked by means of low energy electron diffraction. HOPG (ZYA grade) was cleaved in air just before loading into the preparation chamber and cleaned by *in situ* heating at 400 °C for 15 h. DH6T (H. C. Starck GmbH) and TTC (Aldrich) were evaporated at evaporation rates of about 0.5 Å/min. The nominal film mass thickness (θ) was monitored with a quartz crystal microbalance. Spectra were recorded with a hemispherical electron energy analyzer (VG-CLAM4). UPS spectra were measured using *p*-polarized He I radiation, the angle between incident photons and detected photoelectrons were fixed to 45° with an acceptance angle of ±12°. The spectra were measured at photoelectron takeoff angles (θ_e) of 0° (normal emission) and 45° (off-normal emission). The energy resolution was set to 70 meV. MAES spectra were recorded using He^* ($2\ ^3S$, 19.82 eV). All spectra were measured with the sample biased at −5.00 V. XRR and GID measurements were performed at beamline W1.1 (Ref. 27) at HASYLAB (Hamburg, Germany) under ambient conditions, the wavelength was set to 1.1808 Å. In the GID experiment, an incident angle of the primary beam above the surface plane of α_i=0.15° was chosen, the exit angle above the sample plane α_f was set to 0.5°. The acceptance angle defined by the detector slits was less than 0.3°. The films were prepared analogously to the case of the UPS and MAES measurements (base pressure preparation chamber at 5×10^{-9} mbar). The samples were measured directly after preparation. All preparation steps and measurements were performed at room temperature. The molecular orbitals were calculated using the density functional theory [GAUSSIAN 03 program package (B3LYP/6-311 G*)].[28]

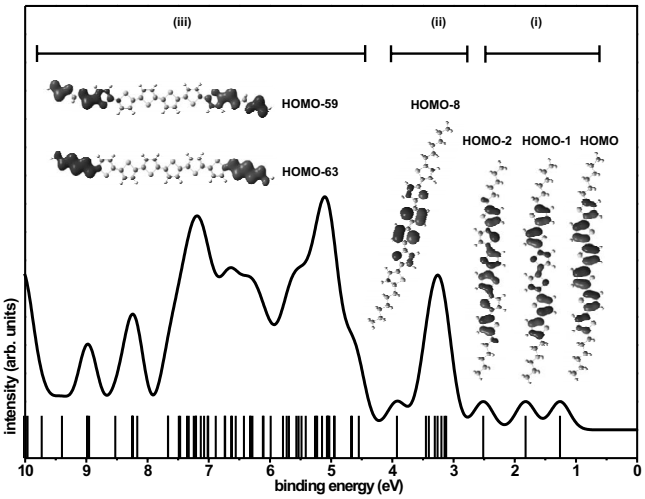

FIG. 1. Energy eigenvalues and a simulated Gaussian broadened spectrum of DH6T. The values are vertically shifted and extended. Some exemplary molecular orbital states are displayed for the regions discussed in the text: (i) HOMO, HOMO-1, HOMO-2, (ii) HOMO-8 (as representative for the localized π-states), (iii) HOMO-59, and HOMO-63 as typical representatives for the hexyl dominated orbitals in the higher BE region.

III. RESULTS

In Fig. 1, the selected molecular orbitals of DH6T, the valence energy eigenvalues, and a simulated Gaussian-broadened DH6T spectrum are shown. The spectrum can be roughly divided into three parts (see Fig. 1): (i) at low BEs comprising delocalized π-orbitals of the conjugated 6T core, consisting of the highest occupied molecular orbital (HOMO), HOMO-1 and HOMO-2, (ii) where it is dominated by six narrowly spaced localized π-states, and (iii) on the high BE side, dominated by σ-states localized mainly on the alkyl chains of DH6T.

Figure 2 shows the UPS and MAES spectra of thickness dependent DH6T on the substrates Ag(111), HOPG, and TTC/Ag(111). The UPS spectra of DH6T/Ag(111) are similar to recently published data.[13,14] However, the shift of the molecular orbitals toward lower BEs, which was attributed to the lying/standing transition of DH6T,[13,14] occurred at higher nominal DH6T coverage in the present study. The spectra of a DH6T film of up to 10 Å nominal thickness showed two molecule derived photoemission features in the low BE region that can be assigned to emission from the LL HOMO and HOMO-1. For the 10 Å coverage, these peaks were centered at 1.95 and 2.60 eV BE, respectively. For lower coverages, these peaks were shifted to lower BEs due to the more efficient screening of the photohole by the electron density of the metal substrate.[8,9] The work function (ϕ) of the pristine Ag(111) surface was determined [using the position of the secondary electron cutoff (SECO)] to 4.55 eV. The deposition of up to 10 Å DH6T, reduced ϕ by 0.90 eV, which is attributed to the electron push-back effect.[8,9] The IE (measured as the difference between the HOMO *maximum* and the vacuum level)[29] for the 10 Å DH6T film was 5.60 eV. Subsequent deposition of DH6T resulted in another photo-

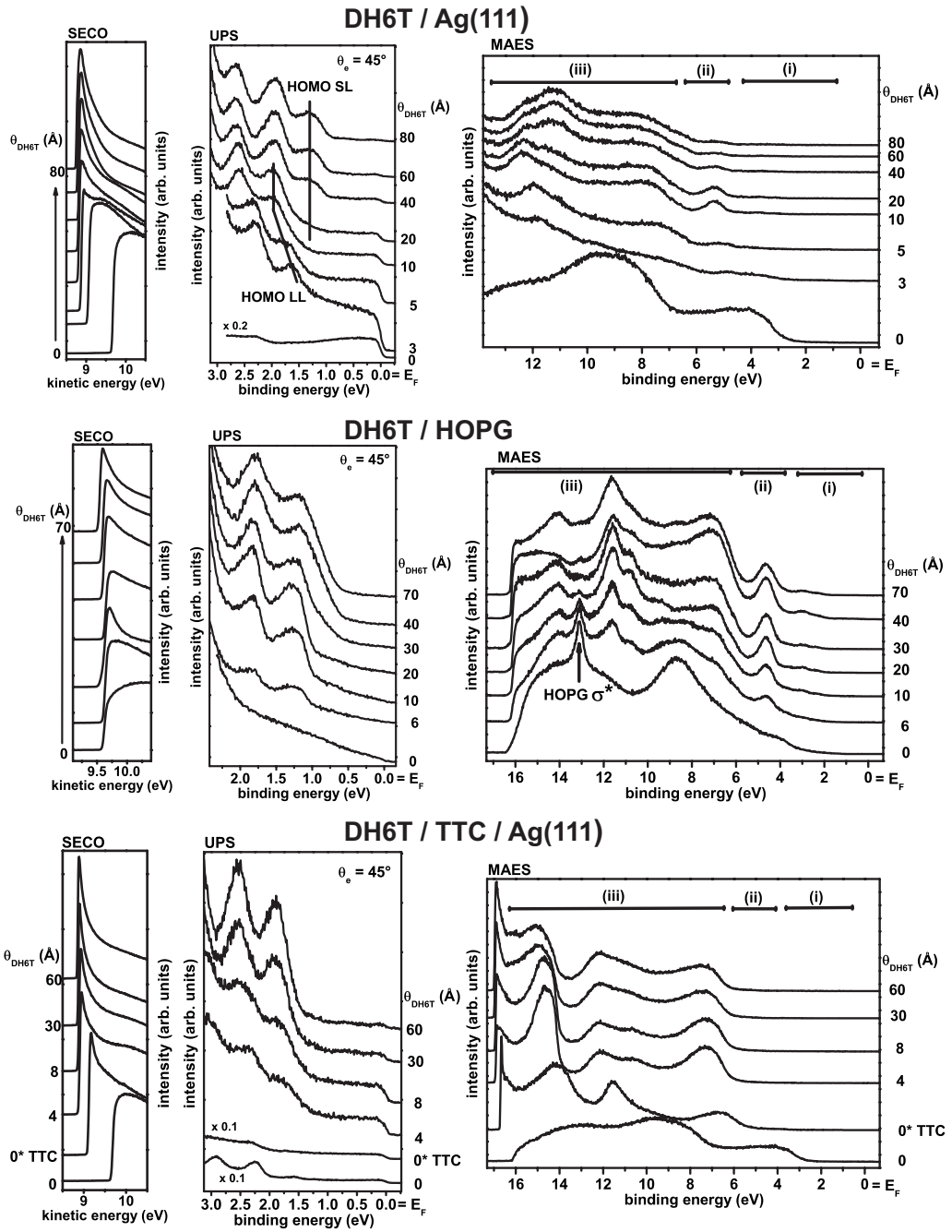

FIG. 2. Spectroscopic results of the thickness series of DH6T on the substrates Ag(111), HOPG, and TTC/Ag(111). Each row displays from left to right the low kinetic energy region with the SECO and the valence electron region of the UPS spectra and the MAES spectra. In the MAES spectra, the regions of π-orbital dominated emission (i) and (ii) and alkyl chain dominated emission (iii) are marked. θ_{DH6T} denotes the nominal DH6T coverage and θ_e the photoelectron takeoff angle. UPS was additionally measured with $\theta_e=0°$ yielding essentially the same results as for $\theta_e=45°$. In the DH6T/Ag(111) UPS spectra, the emission from the HOMO LL and from HOMO SL of DH6T are marked. The label 0^* TTC in the DH6T/TTC/Ag(111) spectra denotes Ag(111) precovered with a monolayer TTC.

emission feature at the low BE side of the former HOMO. This emission feature stems from a layer of standing molecules as deduced from the MAES results where the π-states were not observed (see below). The position of the vacuum level stayed constant during further DH6T deposition. At maximum coverage [80 Å DH6T/Ag(111)], the HOMO was centered at 1.30 eV BE, and HOMO-1 and HOMO-2 were centered at 1.95 and 2.65 eV BE. The IE of SL DH6T was 4.95 eV. In the corresponding MAES spectra, the deposition of up to 10 Å DH6T on Ag(111) caused a suppression of the metal derived features and gave rise to features attributed to organic molecules. HOMO, HOMO-1, and HOMO-2 were hardly resolvable. However, the peak dominated by the six localized π-states centered around 5.30 eV BE was clearly visible. In the higher BE region, several alkyl chain derived peaks appeared. With increasing DH6T coverage, the intensity of the 5.30 eV BE peak increased to a maximum at a film thickness of 10 Å and decreased again for higher coverages.

In the case of DH6T/HOPG the UPS spectra appeared to be qualitatively similar to DH6T/Ag(111) up to a coverage of 20 Å, but the absolute energy positions of the peaks were

different; 1.25 and 1.80 eV BE for HOMO and HOMO-1, respectively. At 20 Å coverage, the peak-width increased, however, without a substantial change in the peak maxima positions. Therefore, the HIB (measured as the difference between the HOMO onset and the Fermi energy) was reduced from 1.00 eV in the monolayer region to 0.60 eV in the multilayer. The vacuum level stayed essentially constant throughout the deposition of DH6T on HOPG, i.e., the IE was 5.70 eV for DH6T/HOPG. In the MAES, the feature at 13.1 eV BE is assigned to a final state structure related to the HOPG σ^* band.[30,31] This feature was visible up to a coverage of 20 Å indicating an incomplete surface coverage even at this high nominal coverage. The MAES spectra exhibited clear features attributed to the adsorbate in the alkyl chain and in the conjugated backbone region for all investigated coverage values. In contrast to DH6T/Ag(111), the intensity of the peak of the localized π-states [region (ii)] was not decreased by increasing DH6T coverage.

In the case of DH6T/TTC/Ag(111), the substrate precoverage by 4 Å TTC decreased ϕ by 0.55 to 4.00 eV. In the valence electron region of the UPS spectra, the metal derived features were suppressed and no features of the saturated TTC were observed in the energy range shown. In the MAES, all Ag(111) derived features were suppressed upon TTC deposition. The spectrum was similar to a reported monolayer TTC spectrum on Ag.[25] Therefore, we conclude that this TTC coverage corresponds to a closed and well-ordered monolayer of TTC on Ag(111).[25] Depositing up to 8 Å DH6T on the TTC precovered Ag(111) substrate resulted in molecule derived features in the UPS spectra very similar to the LL spectra of DH6T on pristine Ag(111), with HOMO and HOMO-1 peaks centered at 1.85 and 2.50 eV BE, respectively. The work function decreased upon DH6T deposition by 0.25 to 3.75 eV; the IE of DH6T was 5.60 eV. The deposition of up to 60 Å DH6T on TTC/Ag(111) did not result in a new emission feature at the low BE side of the monolayer HOMO, in contrast to DH6T on pristine Ag(111). The peaks of the multilayer spectra were slightly sharper than the peaks of the lower coverage spectra. In the MAES, neither the localized π-peak (ii) nor the delocalized π-orbitals (i) of DH6T could be observed in the low BE region for all DH6T coverages. However, in the higher BE region, a clear alkyl chain derived emission was observed.

X-ray diffraction measurements were performed on DH6T films of 48 Å nominal coverage on Ag(111), the results are summarized in Fig. 3. The XRR spectrum exhibits Kiessig fringes[32] at low values of momentum transfer (q_z) that can be attributed to a smooth DH6T film of 36.5 Å thickness. A weak Bragg peak corresponding to a lattice spacing of 3.9 Å is found at q_z=1.62 Å^{-1}. In the GID spectrum, two pronounced peaks at q_{xy} values of 1.749 and 1.990 Å^{-1} could be observed, corresponding to lattice planes perpendicular to the sample surface. The in-plane reflections correspond to lattice spacings of 3.59 and 3.16 Å, which cannot be explained by any reported structures of DH6T.[33–36]

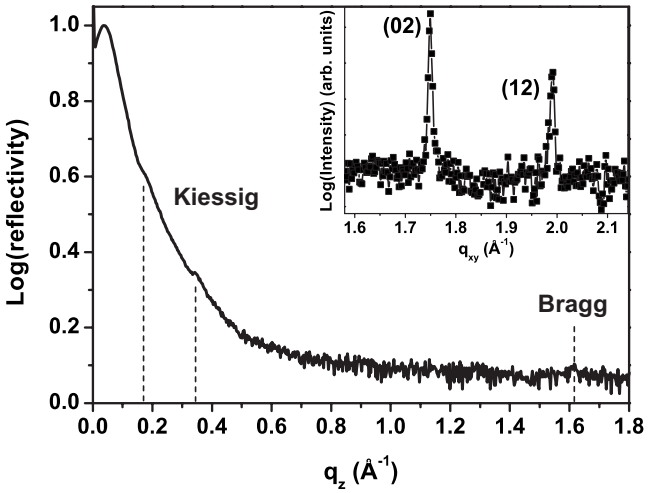

FIG. 3. XRR and GID (inset) spectra of a nominally 48 Å thick DH6T film on Ag(111). XRR exhibits Kiessig fringes corresponding to a film thickness of 36.5 Å at low q_z values and a weak indication of a Bragg peak equivalent to a lattice spacing of 3.9 Å at high q_z, both features are marked with lines. The two pronounced peaks in the GID spectrum (inset) allow to estimate a unit cell for standing DH6T.

IV. DISCUSSION

X-ray diffraction measurements allowed to estimate the unit cell dimensions of DH6T/Ag(111). The vertical thickness of 36.5 Å, derived from the Kiessig fringes in the XRR, is slightly larger than the reported diffraction spacing of 35.5 Å for a DH6T film on SiO_2 composed of molecules tilted by 16° with respect to the substrate.[19] Moreover, the reported unit cell cannot be used to explain the present result from the GID. Our experimental data are not sufficient to derive the unit cell of SL DH6T without additional assumptions since only two in-plane peaks could be observed.[37] However, it is reasonable to assume that the 6T backbone of DH6T adopts a similar packing motif, as in all reported cases of 6T in various environments,[33–36] i.e., a monoclinic unit cell with a herringbone motif. The two 6T polymorphs, in which a unit cell was reported,[35,36] exhibit very different unit cell dimensions but nearly identical unit cell volumes (difference of $<1\%$); a fact, which is also found for other rodlike organic molecules like pentacene,[38–40] where the unit cell volumes of all known polymorphs differ by less than 5%. Therefore, we used the following approach: (i) assume a unit cell volume (V) in the model for the DH6T *backbone* structure close to the reported values of pristine 6T, (ii) find unit cell parameters a and b that allow the indexing of GID peaks with the lowest indices ($hk0$), and (iii) compare the unit cell with the known structures of 6T. Following this approach, we propose as unit cell for the 6T backbone of DH6T: a =6.63 Å, b=7.18 Å, c=22.35 Å, $\beta=(90\pm1)°$, and V =1064 Å^3, which is similar to the unit cell reported by Horowitz *et al.*[36] The two GID peaks can then be assigned to the (020) and (120) reflections, which are also two intense reflections of pristine 6T. Taking into account the film thickness of 36.5 Å derived from the oscillations in the XRR spectrum, we can now model the unit cell dimensions of *standing* DH6T (LL) on *lying* DH6T (SL). The small Bragg peak in the XRR spectrum, corresponding to a lattice spacing of 3.9 Å, is a direct indication for the lying DH6T layer consisting of more than a monolayer since at least two layers are necessary to cause a Bragg diffraction. Through comparison of the structure of α,ω-dihexylquaterthiophene

TABLE I. Unit cell dimensions of the 6T crystal structure, reported by Horowitz *et al.* (transformed to ascending axis dimensions), of the standing phase of the DH6T conjugated backbone and of DH6T/Ag(111). *Z* denotes the number of molecules in the unit cell, *V* is cell volume. The tilt angle between backbone and hexyl chains in the latter case was determined to 28°.

	a (Å)	*b* (Å)	*c* (Å)	β	*Z*	*V* (Å^3)
Horowitz *et al.*[a]	6.029	7.851	44.708	89.24°	4	2116
6T backbone	6.63	7.18	22.25	$(90\pm1)°$	2	1064
DH6T	6.63	7.18	36.5	$(90\pm1)°$	2	1738

[a]Reference 36.

(DH4T),[41] with identical hexyl chain length and reduced backbone dimensions, we can rule out that the thickness oscillations stem from the overall film thickness. This would lead to an unreasonably high mass density of >1.3 g cm^{-3} for the hexyl chains of standing molecules (DH4T at 0.78 g cm^{-3}) as well as to a tilt angle between the backbone and the hexyl chains >60° (DH4T is fully extended). Therefore, we propose the spacing of 36.5 Å to correspond to the (001) lattice spacing (d_{001}) of the DH6T structure, which leads to the following unit cell dimensions of the standing DH6T monolayer: $a=6.63$ Å, $b=7.18$, $c=36.5$ Å, and $\beta=(90\pm1)°$. This leads to a low tilt angle of the alkyl chains of 28° (DH4T is fully elongated), as well as a mass density of ~0.7 g cm^{-3} for the volume occupied by the alkyl chains, which fits the DH4T values well. The unit cell dimensions are summarized in Table I.

For the discussion of the spectroscopic results in relation to the molecular orientation, two main observations have to be considered: (1) the IE derived from the UPS, where the IE strongly depends on the orientation of DH6T and thus provides (indirect) information about the orientation of the molecules, and (2) the intensity of the peak in the MAES spectra, which is dominated by the six narrowly spaced localized π-states at 5 eV BE (ii). In this BE region, no alkyl chain derived states occur. For lying DH6T, both the alkyl chains and the conjugated backbone are accessible for MAES. However, for SL DH6T with the alkyl chains forming the outermost surface, the (localized) π-states of the conjugated part are not accessible. Therefore, we use the intensity of this peak to infer the composition of the exposed sample surface. For comparison, in the case of the DH6T related polymer poly(3-hexylthiophene) (P3HT), the P3HT HOMO is totally suppressed in the MAES spectra if PH3T is in edge-on orientation with the hexyl chains on top. In contrast, if P3HT is in face-on orientation, the P3HT HOMO could be observed.[42]

The system DH6T/Ag(111) acts as a reference system as it has already been investigated before.[13,14] The IE of DH6T is reduced by 0.65 eV from LL to SL (Table II), which is in agreement with the previous work, where a value of 0.55 eV was reported.[13] The intensity reduction of the localized π-state with increasing DH6T coverage in the MAES spectra (Fig. 2) supports an orientational transition of DH6T. As judged from our XRR and GID findings, the transition from lying (LL) to inclined (SL) molecules occurs at a coverage of about two LLs. This is different from the previous work, where this transition occurred at a coverage of one LL.[13]

Although nominally equal Ag(111) single crystals were used in both studies, which should have the same physical properties, slight differences in the surface properties, such as varying terrace sizes or step edge densities, can have a significant impact on organic thin film growth.[5,6] In fact, we expect that the crystals did not exhibit exactly the same surface morphology, as the work functions of the pristine crystals were slightly different, $\phi=4.40$ eV (Ref. 13) and $\phi=4.55$ eV (this study). Moreover, the preparation conditions of an organic thin film may differ to some extent in the two experimental setups. In particular, small changes in the substrate temperature during film growth (which was not precisely controlled in both experiments) can heavily influence the growth of organic thin films.[43–45]

A schematic of DH6T/Ag(111) is presented in Fig. 4. The island growth mode of multilayers is concluded from the MAES spectra, as the peak of the localized π-states (ii) does not vanish completely even for thick films. In case of layer-by-layer or the Stranski–Krastanov growth of SL, this peak would not be observable due to the alkyl chains forming the sample surface. The exact LL structure is unknown, but our UPS and x-ray diffraction results point to two LLs. The structure of LL DH6T was determined on Au(111) by scanning tunneling microscopy (STM).[46] We speculate on an

TABLE II. Ionization energies (in eV) of a double layer and multilayers coverage of DH6T on the respective substrates. The values are measured from the HOMO *maxima* to the vacuum level.

	Ag(111)	HOPG	TTC/Ag(111)
Double layer	5.60	5.70	5.60
Multilayer	4.95	5.70	5.60

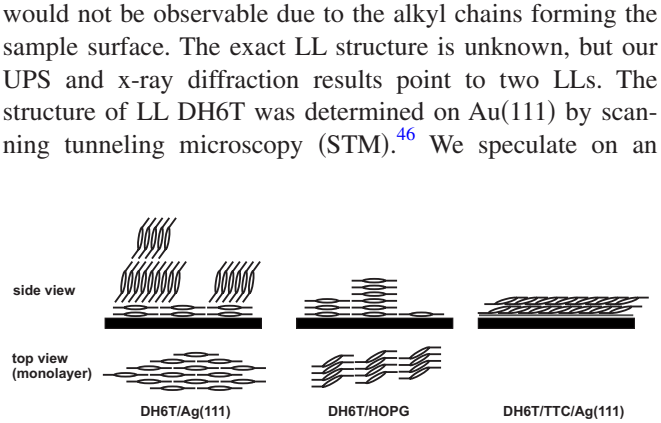

FIG. 4. Proposed growth models of DH6T on the investigated substrates. The structure of the side views is determined by XRR, GID, UPS and MAES for DH6T/Ag(111), for HOPG as substrate DH6T is assumed to adopt the bulk phase (Ref. 19), the structure of DH6T/TTC/Ag(111) is concluded from UPS and MAES and is one specific of several possible models. The top views for DH6T/Ag(111) (Ref. 46) and DH6T/HOPG (Ref. 47) are taken from literature.

analogous structure on Ag(111). Monolayers of unsubstituted 6T on Au(111) and Ag(111) exhibit rather similar structures.[21,46–48]

For DH6T on HOPG, no substantial changes could be observed between thinner and thicker films in both the UPS and MAES spectra. With increasing film thickness, no shift of the HOMO and HOMO-1 peak maxima were observed. Therefore, changes in the molecular orientation as found for DH6T/Ag(111) are unlikely. The IE of DH6T/HOPG is close to the IE of LL DH6T/Ag(111) (Table II). In addition, the localized π-peak in the MAES spectra (Fig. 2) was visible for all DH6T coverages. Therefore, we propose lying DH6T in the monolayer and the multilayer regime on HOPG. This finding is supported by the STM data of DH6T/HOPG.[47] The structure of the lying monolayer phase of DH6T/HOPG measured with STM in a solution[47] resembles a cleavage plan of the bulk structure of DH6T,[19] which contains the backbone long molecular axis. Thus, it seems plausible that DH6T can grow in its bulk phase from monolayer coverage onward on HOPG. A model of DH6T/HOPG is shown in Fig. 4, where the orientation and conformation is adapted from literature.[19,47] We conclude the growth in the Stranski–Krastanov mode from the MAES, where up to a coverage of 20 Å (which is clearly more than a nominal lying monolayer), the HOPG σ^* signal can be observed, where it vanishes only for higher coverages.

The IE of DH6T/TTC/Ag(111) (Table II) indicates a lying orientation of DH6T. However, in the MAES, no peaks originating from the conjugated part of the molecules are observed, i.e., MAES results point to the standing molecules. Therefore, we have to develop an alternative molecular orientation/conformation model, which differ from the "simple" standing or lying DH6T. Our XRR and GID results together with literature[19,41] clearly show that the tilt angle between the alkyl chains and the conjugated backbone is variable, i.e., DH6T grown on a solid can change its orientation and conformation. Close inspection of the MAES spectra of multilayer films of DH6T on Ag(111) and on TTC/Ag(111) reveal differences in the part specific for emission from the alkyl chains (Fig. 2). In literature the influence of alkane orientation on the MAES spectra has been discussed in detail.[49,50] The hesitant increase in the hexyl derived emission intensity on the low BE range (around 6 eV BE) for DH6T/Ag(111) is typical for almost standing alkyls,[50] as corroborated by XRR and GID, whereas the rapid increase of the hexyl emission intensity in the same part of the spectra of multilayers DH6T/TTC/Ag(111) points to almost lying alkyls.[49] Thus, we assume that for DH6T/TTC/Ag(111): (i) almost lying 6T backbones (from IE), (ii) lying alkyl chains (from the alkyl MAES emission), and (iii) only alkyl chains forming the uppermost surface (no π-dominated peak around 5 eV BE in the MAES spectra). Deviations of the proposed orientation are possible, since the spectroscopic methods, UPS, and MAES only gives molecular orientations with low accuracy. Indeed, little tilt angles of the DH6T components can lead to a possible growth model which accomplishes all assumptions (Fig. 4). The structure of DH6T/TTC/Ag(111) is highly different to the structure of SL DH6T/Ag(111), although a similar orientation and conformation of DH6T was expected on the pure alkanes of TTC, since the alkyl chains within the LL DH6T were claimed to be responsible for the standing up process of DH6T. However, the measured orientation and conformation of DH6T on TTC/Ag(111) favors reasonably a face on face overlap of the DH6T hexyl chains with the TTC alkanes.

V. CONCLUSIONS

For DH6T/Ag(111), an orientational transition from lying molecules in the monolayer to standing molecules in multilayers was confirmed. The IE of DH6T is 0.65 eV lower for standing molecules. In addition, x-ray diffraction experiments allowed to estimate the unit cell of standing DH6T on lying DH6T on Ag(111) to be $a=6.63$ Å, $b=7.18$, $c=36.5$ Å, and $\beta=(90\pm1)°$. On HOPG, no monolayer/multilayer transition occurs. In contrast, the weak molecule-HOPG interaction allows DH6T to grow in the bulk phase with lying molecules already from monolayer coverage onward. For DH6T/TTC/Ag(111), the orientation and conformation of DH6T is again different, in this case, the DH6T alkyl chains are flat lying, whereas the conjugated backbone is slightly inclined. However, no change in the orientation between monolayer and multilayer coverage was observed. Notably, the molecular orientation and conformation of the DH6T multilayer on Ag(111) and of DH6T/TTC/Ag(111) is very different. We, thus, demonstrated that simple prepatterning of metal substrates with saturated alkyl chains cannot induce growth of standing DH6T with a reduced barrier for hole injection from the metal substrate. Therefore, alternative approaches to control molecular orientation and charge injection barriers in organic electronic devices have to be explored.

ACKNOWLEDGMENTS

The authors thank H. C. Starck GmbH for providing DH6T. We thank R. L. Johnson and W. Caliebe (HASYLAB, Hamburg, Germany) for experimental support during synchrotron work. N.K. acknowledges financial support from the Emmy-Noether-Program (DFG), SD by the German Academic Exchange Service (DAAD) and IS by the Sonderforschungsbereich 448 (DFG). This work was supported in part by the 21st Century COE Program of MEXT (Frontiers of Super-Functionality Organic Devices, Chiba University).

[1] X. L. Chen, A. J. Lovinger, Z. Bao, and J. Sapjeta, Chem. Mater. **13**, 1341 (2001).
[2] P. Sreearunothai, A. C. Morteani, I. Avilov, J. Cornil, D. Beljonne, R. H. Friend, R. T. Phillips, C. Silva, and L. M. Herz, Phys. Rev. Lett. **96**, 117403 (2006).
[3] N. Koch, A. Elschner, J. Schwartz, and A. Kahn, Appl. Phys. Lett. **82**, 2281 (2003).
[4] H. Sirringhaus, P. J. Brown, R. H. Friend, M. M. Nielsen, K. Bechgaard, B. M. W. Langeveld-Voss, A. J. H. Spiering, R. A. J. Janssen, E. W. Meijer, P. Herwig, and D. M. de Leeuw, Nature (London) **401**, 685 (1999).
[5] G. Witte and C. Wöll, J. Mater. Res. **19**, 1889 (2004).
[6] D. E. Hooks, T. Fritz, and M. D. Ward, Adv. Mater. (Weinheim, Ger.) **13**, 227 (2001).
[7] N. Koch, ChemPhysChem **8**, 1438 (2007).
[8] A. Kahn, N. Koch, and W. Y. Gao, J. Polym. Sci., Part B: Polym. Phys. **41**, 2529 (2003).
[9] H. Ishii, K. Sugiyama, E. Ito, and K. Seki, Adv. Mater. (Weinheim, Ger.) **11**, 605 (1999).

[10]N. Koch, I. Salzmann, R. L. Johnson, J. Pflaum, R. Friedlein, and J. P. Rabe, Org. Electron. **7**, 537 (2006).
[11]H. Fukagawa, H. Yamane, T. Kataoka, S. Kera, M. Nakamura, K. Kudo, and N. Ueno, Phys. Rev. B **73**, 245310 (2006).
[12]J. Ivanco, B. Winter, F. P. Netzer, and M. G. Ramsey, Adv. Mater. (Weinheim, Ger.) **15**, 1812 (2003).
[13]S. Duhm, H. Glowatzki, J. P. Rabe, N. Koch, and R. L. Johnson, Appl. Phys. Lett. **88**, 203109 (2006).
[14]S. Duhm, G. Heimel, I. Salzmann, H. Glowatzki, R. L. Johnson, A. Vollmer, J. P. Rabe, and N. Koch, Nat. Mater. **7**, 326 (2008).
[15]N. Koch and A. Vollmer, Appl. Phys. Lett. **89**, 162107 (2006).
[16]H. Fukagawa, S. Kera, T. Kataoka, S. Hosoumi, Y. Watanabe, K. Kudo, and N. Ueno, Adv. Mater. (Weinheim, Ger.) **19**, 665 (2007).
[17]M. Halik, H. Klauk, U. Zschieschang, G. Schmid, S. Ponomarenko, S. Kirchmeyer, and W. Weber, Adv. Mater. (Weinheim, Ger.) **15**, 917 (2003).
[18]J.-O. Vogel, I. Salzmann, R. Opitz, S. Duhm, B. Nickel, J. P. Rabe, and N. Koch, J. Phys. Chem. B **111**, 14097 (2007).
[19]F. Garnier, A. Yassar, R. Hajlaoui, G. Horowitz, F. Deloffre, B. Servet, S. Ries, and P. Alnot, J. Am. Chem. Soc. **115**, 8716 (1993).
[20]C. E. Heiner, J. Dreyer, I. V. Hertel, N. Koch, H.-H. Ritze, W. Widdra, and B. Winter, Appl. Phys. Lett. **87**, 093501 (2005).
[21]G. Yoshikawa, M. Kiguchi, S. Ikeda, and K. Saiki, Surf. Sci. **559**, 77 (2004).
[22]Y. Harada, S. Masuda, and H. Ozaki, Chem. Rev. (Washington, D.C.) **97**, 1897 (1997).
[23]S. Kera, H. Setoyama, M. Onoue, K. K. Okudaira, Y. Harada, and N. Ueno, Phys. Rev. B **63**, 115204 (2001).
[24]M. Yamamoto, Y. Sakurai, Y. Hosoi, H. Ishii, K. Kajikawa, Y. Ouchi, and K. Seki, J. Phys. Chem. B **104**, 7370 (2000).
[25]E. Ito, H. Oji, H. Ishii, K. Oichi, Y. Ouchi, and K. Seki, Chem. Phys. Lett. **287**, 137 (1998).
[26]H. Yamane, H. Fukagawa, S. Nagamatsu, M. Ono, S. Kera, K. K. Okudaira, and N. Ueno, IPAP Conf. Ser. **6**, 19 (2005).
[27]S. Schiefer, M. Huth, A. Dobrinevski, and B. Nickel, J. Am. Chem. Soc. **129**, 10316 (2007).
[28]M. J. Frisch, G. W. Trucks, H. B. Schlegel *et al.*, GAUSSIAN 03, Revision C.02, Gaussian, Inc., Wallingford, CT, 2004.
[29]Often the IE is defined by the difference of the vacuum level and the HOMO onset. However, to allow for a better comparability of the values found on the different substrates irrespective of the broadening of the HOMO peaks, we have chosen a different definition in this work.
[30]S. Masuda, H. Hayashi, and Y. Harada, Phys. Rev. B **42**, 3582 (1990).
[31]T. Takahashi, H. Tokailin, and T. Sagawa, Phys. Rev. B **32**, 8317 (1985).
[32]H. Kiessig, Ann. Phys.-Berlin **402**, 769 (1931).
[33]B. Servet, S. Ries, M. Trotel, P. Alnot, G. Horowitz, and F. Garnier, Adv. Mater. (Weinheim, Ger.) **5**, 461 (1993).
[34]J. Bernstein, J. A. R. P. Sarma, and A. Gavezzotti, Chem. Phys. Lett. **174**, 361 (1990).
[35]T. Siegrist, R. M. Fleming, R. C. Haddon, R. A. Laudise, A. J. Lovinger, H. E. Katz, P. Bridenbaugh, and D. D. Davis, J. Mater. Res. **10**, 2170 (1995).
[36]G. Horowitz, B. Bachet, A. Yassar, P. Lang, F. Demanze, J.-L. Fave, and F. Garnier, Chem. Mater. **7**, 1337 (1995).
[37]We exclude that the reflections found in GID stem from lying DH6T molecules since (i) the corresponding lattice spacings are far below the extensions of the DH6T molecule and (ii) no peak at low momentum transfer could be observed.
[38]C. C. Mattheus, G. A. de Wijs, R. A. de Groot, and T. T. M. Palstra, J. Am. Chem. Soc. **125**, 6323 (2003).
[39]M. Oehzelt, R. Resel, C. Suess, R. Friedlein, and W. R. Salaneck, J. Chem. Phys. **124**, 054711 (2006).
[40]D. Nabok, P. Puschnig, C. Ambrosch-Draxl, O. Werzer, R. Resel, and D.-M. Smilgies, Phys. Rev. B **76**, 235322 (2007).
[41]M. Moret, M. Campione, A. Borghesi, L. Miozzo, A. Sassella, S. Trabattoni, B. Lotz, and A. Thierry, J. Mater. Chem. **15**, 2444 (2005).
[42]X. T. Hao, T. Hosokai, N. Mitsuo, S. Kera, K. Mase, K. K. Okudaira, and N. Ueno, Appl. Phys. Lett. **89**, 182113 (2006).
[43]F. Biscarini, R. Zamboni, P. Samorí, P. Ostoja, and C. Taliani, Phys. Rev. B **52**, 14868 (1995).
[44]M. A. Loi, E. Da Como, F. Dinelli, M. Murgia, R. Zamboni, F. Biscarini, and M. Muccini, Nat. Mater. **4**, 81 (2005).
[45]R. Ruiz, D. Choudhary, B. Nickel, T. Toccoli, K.-C. Chang, A. C. Mayer, P. Clancy, J. M. Blakely, R. L. Headrick, S. Iannotta, and G. G. Malliaras, Chem. Mater. **16**, 4497 (2004).
[46]H. Glowatzki, S. Duhm, K.-F. Braun, J. P. Rabe, and N. Koch, Phys. Rev. B **76**, 125425 (2007).
[47]A. Stabel and J. P. Rabe, Synth. Met. **67**, 47 (1994).
[48]M. Kiel, K. Duncker, C. Hagendorf, and W. Widdra, Phys. Rev. B **75**, 195439 (2007).
[49]H. Ozaki and Y. Harada, J. Am. Chem. Soc. **112**, 5735 (1990).
[50]S. P. Chenakin, B. Heinz, and H. Morgner, Surf. Sci. **397**, 84 (1998).